Earth Syst. Dynam. Discuss., https://doi.org/10.5194/esd-2017-114
Manuscript under review for journal Earth Syst. Dynam.
Discussion started: 18 December 2017

Earth System Dynamics Discussions

Moisture transport and Antarctic sea ice: Austral spring 2016 event

Monica Ionita[1], Patrick Scholz[1], Klaus Grosfeld[1], Renate Treffeisen[1]

[1]Alfred Wegener Institute Helmholtz Centre for Polar and marine Research, Bremerhaven, 27570, Germany

Correspondence to: Monica Ionita (Monica.ionita@awi.de)

Abstract. In austral spring 2016 the Antarctic region experienced anomalous sea ice retreat in all sectors, with sea ice extent in October and November 2016 being the lowest in the Southern Hemisphere over the observational record (1979 – present). The extreme sea ice retreat was accompanied by widespread warming along the coastal areas as well as in the interior of the Antarctic continent. This exceptional event occurred along with a strong negative phase of the Southern Annular Mode (SAM) and the wettest and warmest spring on record, over large areas covering the Indian ocean, the Ross Sea and the Weddell Sea. In October 2016, the positive anomalies of the totally integrated water vapor (IWV) and 2m air temperature (TT) over the Indian Ocean, Western Pacific, Bellingshausen Sea and southern part of Ross Sea were unprecedented in the last 39 years. In October and November 2016, when the lowest daily sea ice concentration anomalies were observed, repeated episodes of poleward advection of warm and moist air took place, with the most intense episode occurring at the end of November 2016. These results suggest the importance of moist and warm air intrusions into the Antarctic region as one of the main contributors to this exceptional sea ice retreat event.

1 Introduction

Sea ice in both polar regions is an important indicator for the expression of global climate change and its polar amplification. It also plays an important role in modulating the global climate system by influencing the atmospheric and oceanic circulations. Moreover, it has also a strong impact on the global economic system through changes in marine and natural resources development. Consequently, a broad scientific as well as societal interest exists on sea ice, its coverage, variability, and long term change (National Research Council, 2012). Recent observed changes in the Artic have become the "face" for global climatic changes, especially due to the rapidly decreasing trend of the summer sea ice extent over the last two decades (Serreze and Stroeve, 2015). The trends in the Arctic sea-ice extent are negative for all months, with the largest trend recorded at the end of the melt season in September (Serreze et al., 2007; Stroeve et al., 2015), with an average decline of 12.9% per decade relative to the long-term mean of 1981 – 2010 September average (Grosfeld et al., 2016).

In contrast, over the Antarctic region the sea ice extent shows an increasing trend, seemingly at odds with climate model projections. The increase in the Antarctic sea ice extent can be largely explained by natural climate fluctuations (Meehl et al., 2016), linked with different factors/drivers like: atmospheric temperature or wind stress (Liu et al., 2004; Turner et al., 2009; Lefebvre and Goosse, 2005), precipitation (Liu and Curry, 2010), ocean temperature (Jacobs and Comiso, 1997), and feedbacks in the atmosphere or ocean (Stammerjohn et al., 2012; Zhang, 2007). Antarctica experienced a complete change,

Earth Syst. Dynam. Discuss., https://doi.org/10.5194/esd-2017-114
Manuscript under review for journal Earth Syst. Dynam.
Discussion started: 18 December 2017

featuring negative sea ice extent anomalies from September 2016 until April 2017. This shift in the sea ice extent variability could be caused either by a potential change of the long term trend or by natural climate variability (Turner et al., 2017).

Whereas the coupled atmosphere-ocean-sea ice models, which are driven by realistic natural and anthropogenic forcing, are able to replicate the decreasing Arctic trend (Stroeve et al., 2012), they also have the tendency to simulate a significant decrease in Antarctic sea ice cover (Turner et al., 2013), in contrast with the observed increasing trend. Shu et al. (2015) showed that only one out of seven CMIP5 models is able to simulate the sign of the Antarctic sea ice trend correctly. As the confidence on numerical simulations relies on an adequate representation of the late-twentieth-century changes (Colins et al., 2014), the understanding of the physical processes generating the Antarctic sea ice extent (SIE) trend and variability is crucial for the relevance of the projected Southern Hemisphere sea ice extent decrease. As the Antarctic SIE increasing trend is not simulated properly by the general circulation models (Shu et al., 2015), the analyses of observed, reconstructed, and reanalysis data are critical for the investigation of its causes. In this respect, here we analyze the exceptional Antarctic austral spring of 2016 from a climatological point of view. The objectives of our paper are as follows: (a) to characterize the temporal and spatial extent of the spring 2016 exceptional sea ice melting event using both daily and monthly sea ice data; (b) to analyze the key drivers of the event, with a special emphasis on the role played by enhanced moisture transport and warm intrusions into the Antarctic region; (c) to place the austral spring 2016 into a long-term perspective. The paper is structured as follows: in Section 2, we introduce the data used in this study; the main results of our analysis are shown in Section 3, while the concluding remarks are presented in Section 4.

2 Data and methods

2.1 Data

For the daily sea ice concentration (SIC) we utilize, the passive microwave sea ice concentration processed using the National Snow and Ice Data Center (NSIDC) bootstrap algorithm (Comiso and Nishio, 2008; Meier et al., 2013) over the period 1979 – 2016. Prior to 1987, data are only available every other day, hence data for missing days were produced by linear interpolation for each pixel between the fields of the previous and next days. The monthly SIE index (Fetterer et al., 2016) over the Antarctic region has been extracted from the NSIDC ftp server (ftp://sidads.colorado.edu/DATASETS/NOAA/G02135/north/). Sea ice extent is defined as the total area of all satellite pixels where the sea ice concentration equals or exceeds 15%. Following previous studies (Zwally et al., 2002; Turner et al., 2017), we examine the anomalies of the daily and monthly SIC and SIE for the Southern Ocean as a whole and for five separate sectors (Figure 1): the Ross Sea (RS) (160°E–130°W), Amundsen-Bellingshausen Sea (ABS) (130°W–60°W), Weddell Sea (WS) (60°W–20°E), Indian Ocean (IO) (20°E–90°E), and western Pacific Ocean (WPO) (90°E–160°E).

For the Southern Hemisphere (SH) temperature and atmospheric circulation, we use the monthly means of air temperature at 2m (TT), zonal wind at 10 m (U), meridional wind at 10 m (V), mean sea level pressure (SLP), the vertical integral of water

vapor (IWV), the vertical integral of eastward water vapor flux, and the vertical integral of northward water vapor flux from the European Centre for Medium-range Weather Forecasts (ECMWF) Interim (ERA-Interim) reanalysis fields (Dee et al., 2011). ERA-Interim uses a four-dimensional variational assimilation scheme with a twelve-hour analysis window. The data assimilation system is based on a 2006 version of the ECMWF Integrated Forecast Model. The spatial resolution of the model is T255 (~80 km) on 60 vertical levels from the surface up to 0.1 hPa (Dee et al., 2011). The data are continuously updated in real time from 1st January 1979. The ERA-Interim fields are reliable across high southern latitudes from 1979 and are considered to be the best reanalysis data set for depicting recent Antarctic climate (Bracegirdle and Marshall, 2012).

The station based monthly mean temperature data has been extracted from the REference Antarctic Data for Environmental Research (READER). The primary sources of data are the Antarctic research stations and automatic weather stations. The stations used in the current study have been downloaded from the following website: https://legacy.bas.ac.uk/met/READER/data.html.

For the Southern Annular Mode (SAM) index, we used the index from https://legacy.bas.ac.uk/met/gjma/sam.html. SAM index is available over the period 1957 up to date and the index is computed from surface meteorological observations from Antarctic coastal and Southern Ocean island stations (Marshall, 2003). All the anomalies (SIC, SLP, TT, IWV) used in this study were computed relative to the climatological period 1981–2010.

2.2 Methods

The *stability maps* approach used in this study is based on a methodology that was successfully applied to predict the monthly to seasonal streamflow of Elbe and Rhine rivers (Ionita et al., 2008, 2015, 2017; Meißner et al., 2017). The basic idea of the stability maps is to identify regions with stable teleconnections (the correlation does not change on time) between SIE averaged over specific regions (e.g. IO, WS) and meteorological/climatological gridded data (e.g. IWV, TT). As such, we correlate the regional sea ice index with IWV and TT gridded fields in a 21-years moving window. The correlation is considered to be *stable* for those grid points where the sea ice index and the gridded fields are significantly correlated at 95%, 90%, 85%, and 80% significance level, for more than 80% of the 21-years moving windows. The regions where the correlation is positive and stable will be represented as dark red (95% significance level), red (90% significance level), orange (85% significance level) and yellow (80% significance level) on the stability maps (see Figure 4 and Figure 5). The regions where the correlation between the regional SIE index and the gridded data is stable and negative will be represented as dark blue (95% significance level), blue (90% significance level), green (85% significance level) and light green (80% significance level) on the stability maps (see Figure 4 and Figure 5). The results remain qualitatively the same if the length of the moving window varies between 15 and 25 years. A more detailed description of the *stability maps* approach can be found in Ionita et al. (2008, 2017).

Earth Syst. Dynam. Discuss., https://doi.org/10.5194/esd-2017-114
Manuscript under review for journal Earth Syst. Dynam.
Discussion started: 18 December 2017

3 Results

3.1 Daily and monthly Antarctic sea ice extent

Antarctic sea ice has shown increased SIE, area ,and concentration from the late 1970's until 2015. Even though the trend itself is modest (Yuan et al., 2017), it is somewhat problematic in the context of the overall global warming signal. When looking at the SIE anomalies over the last 38 years, the first 8 months of 2016 are not particularly anomalous (not shown). Both July (Figure S1a) and August (Figure S1b) 2016 were characterized by slightly positive SIE anomalies over the whole Antarctic region. However, starting from September 2016, the situation changed dramatically. The Antarctic SIE from September 2016 until December 2016 was characterized by significant negative anomalies, with November 2016 and December 2016 ranking as the lowest SIE for those respective months in the sea ice record (Figure S1). November mean SIE was over 5 standard deviation below the 1981-2010 average (Stammerjohn and Scambos, 2017). September 2016 ranks as the 7th in term of lowest SIE on record, while October 2016 ranks as the second in terms of lowest SIE.

To have a clear picture of the spatial pattern of the extreme events in the austral spring 2016, we have computed the SIC anomalies in each grid point, from September 2016 until December 2016 (Figure 1). In September 2016, most of the Antarctic region was characterized by negative SIC anomalies (Figure 1a), with some exceptions over the western part of the WS and the western part of RS, where positive SIC anomalies prevailed. The same spatial pattern was present also in October 2016 (Figure 1b), but with much higher amplitudes (SIC anomalies < 40%) over the IO, WS, and the eastern part of RS. In November 2016, the negative SIC anomalies become very high in amplitude over the eastern part of the WS and western part of ABS (Figure 1c). Weak positive SIC anomalies were present over the western part of WS, as well as strong positive SIC anomalies over the northern part of RS, and ABS. Over the WPO, the SIC anomalies reversed their sign (negative to positive) in November 2016. In December 2016, the whole RS was characterized by negative SIC anomalies (Figure 1d), as well as ABS (with some small exceptions over the eastern part) and IO.

When looking at the daily evolution of the SIE anomalies throughout the austral spring 2016, some very particular features are present. In September 2016, most of the negative SIE anomalies at the Antarctic level were mainly driven by the daily sea ice extent anomalies over IO, ABS, and WPO (Figure S2 and Figure S3). Over the Ross Sea the daily sea ice extent anomalies were positive throughout the whole September 2016. In October 2016, all the regions, except Weddell Sea, were characterized by daily negative SIE anomalies, especially IO. The situation became very dramatic in November 2016, when daily negative SIE anomalies were recorded over all the analysed regions (Figure S2 and Figure S3), especially IO and WS. The combined effect of all the regions showing daily negative sea ice extent anomalies throughout all November 2016 was a SIE anomaly of more than 2.2 mil. km^2 around 20th of November. In December 2016, the extreme daily anomalies continued the decreasing trend, with more than 2.7 mil. km^2 of negative SIE anomalies occurring in the middle of the month. Most of the contribution for the extreme sea ice extent anomalies in December 2016, was coming from the WS. By analysing the daily SIE anomalies throughout the year 2016, one of the most striking feature is the abrupt drop of more than 1.7 mil. km^2

of sea ice extent from the beginning of November 2016 until the middle of December 2016, which is unprecedented since the beginning of the 1980 (not shown).

3.2 Climatological analysis of the austral spring 2016

In September 2016, the atmospheric circulation was reminiscent to the zonal wave number three and projected onto the positive phase of SAM (Figure 2a), with a center of negative SLP anomalies over the Antarctic continent flanked by three centers of positive SLP anomalies: one over the RS, one over IO, and one over WS. SAM had a value of +2.46 in September 2016, which ranks as the fourth highest value on record, since 1958. This SLP pattern was associated with positive temperature anomalies over the ABS, WS, IO, and eastern WS and negative temperature anomalies over most of the Antarctic continent, except the Antarctic Peninsula (Figure 2b). The three positive SLP centers were positioned in such a way that they enhanced poleward advection of warm and moist air, especially over IO, eastern RS, WS, and Bellingshausen Sea (Figure 2c). The areas characterized by positive temperature anomalies and enhanced water vapor correspond to the regions were the negative SIC anomalies were occurring in September 2016 (see Figure 1a).

In October 2016, the atmospheric circulation was more meridional and wavier, with altering positive and negative SLP anomalies surrounding the Antarctic continent (Figure 2d). SAM had a value of -0.89, ranking as the 14th lowest SAM index on record. This wavy SLP pattern favored, again, the advection of warm (Figure 2e) and moist air (Figure 2f) towards the continent and the coastal areas, the most affected regions, in terms of sea ice reduction, corresponding to the regions where warm and moist intrusions occurred: WS, IO, ABS, and western WPO. October 2016 was also characterized by widespread warming along the coastal areas as well as in the interior of the continent, with some small exceptions. In November 2016, SAM index dropped to a value of -3.12, which ranks as the fifth lowest SAM index since 1958. In terms of large-scale atmospheric circulation, an anomalous high pressure system developed over the polar cap, which resulted in the weakening of the westerlies. The high pressure system over the polar cap was surrounded by a band of negative SLP anomalies, stretching from IO – WPO - RS up to ABS (Figure 2g). The weakening of the westerlies resulted in extreme positive temperature anomalies over the whole polar cap and the coastal areas (Figure 2h). Moreover, over ABS, WS, and RS, enhanced advection of warm and moist air from the lower latitudes led to a rapid melting of the sea ice over these regions (Figure 1c and Figure 2i).

In December 2016, the atmospheric circulation was similar to that of November 2016: high pressure system over the polar cap, surrounded by negative SLP anomalies over WS and IO (Figure 2j). The December value of the SAM index (-1.52, 10th lowest for December since 1957) was much smaller compared to November 2016. This is visible also in the amplitude of the SLP anomalies, over the polar cap, between the two months, with December 2016 featuring weaker (in amplitude) positive SLP anomalies over the Antarctic Continent and smaller temperature anomalies (by a factor of 4 between November 2016 and December 2016). In December 2016, positive (but weak) temperature anomalies prevailed over most of the Antarctic

Continent, except for the central part. Positive temperature anomalies (Figure 2k) and wet conditions (Figure 2l) were also recorded over RS and parts of the coastal regions of IO and WPO.

3.3 Long-term context of the austral spring 2016 event

To prove that austral spring 2016 was a very particular year in terms of reduced SIC and warm and wet conditions over the Antarctic region and the surrounding areas, we have computed the rank maps for the monthly (September – December) SIC (Figure 3 – first column), IWV (Figure 3 – middle column), and TT (Figure 3 – third column). The rank maps are computed to emphasize how exceptional was 2016 in a long term context (1979 – 2016). The red areas in Figure 3 indicate that 2016 was the year with the lowest SIC, the wettest, and the warmest on record, over the period 1979 – 2016. The orange colors indicate that 2016 was the second lowest SIC, wettest, and warmest and so on. We have chosen only the top 5 ranks, to be able to clearly capture how exceptional the year 2016 was. The idea of ranking maps has been successfully used before to emphasize the "exceptionality" of a particular year/season/month (Ionita et al., 2017).

Figures 3a, b, and c indicate that September 2016 was the month with the lowest SIC over distinct areas in the WS, RS, and ABS, and ranks among the top five years with the lowest SIC over an extended band in the central IO (Figure 3a). The regions with the lowest SIC, in September 2016, were also the wettest (Figure 3b) and warmest (Figure 3c) on record. The regions with the lowest SIC extent, in October 2016, are similar to the ones from September 2016, but the spatial extent of low SIC anomalies is larger when compared to September 2016 (Figure 3d). October 2016 stands out as the wettest and warmest year on record over large areas covering the surroundings of the Antarctica: almost the entire IO region stands out as the wettest and warmest on record, with small exceptions in the western part of it; the southern part of RS was also among the wettest and warmest regions on record, while the whole Bellingshausen Sea stands out in the first five wettest and warmest October on record (Figure 3e and f). The largest regions affected by low SIC were recorded in November 2016 (Figure 3g), with central IO, south-eastern RS, and small parts of WS being the areas with the lowest SIC on record. In terms of wet and warm, the regions that stand out as very extreme, in November 2016, are located over the eastern part of RS, and the south-eastern part of the Antarctica as well as over the WS (Figure 3h and i). Around the coastal areas of East Antarctica, all the stations where measurements are available recorded the highest monthly mean temperatures in October and November 2016 (Casey: -3.7°C; Davis: -2.2°C, Syowa: -4.7°C, Figure 4a and 4b) (Keller et al., 2017). In December 2016, the spatial extent of the extreme low SIC is much smaller (Figure 3j) compared to the previous months, being restricted just to the southern part of RS and eastern part of ABS. The same is valid for IWV and TT. The north-western part of RS ranks as the wettest on record (Figure 3k), while small regions in WS rank as the warmest on record (Figure 3l).

3.4 Long term relationship between regional Antarctic sea ice and moisture availability and temperature

As it was shown in Section 3.3, the period October- December 2016 was characterized by extreme warm temperatures and enhanced moisture covering large areas in the Antarctic region (Figure 2). To examine the relationship between moisture and temperature on one hand and the regional Antarctic sea ice variability on the other hand, from a long term perspective, we

have computed the stability maps between November IO SIE and October and November IWV and TT, as well as the stability maps between December RS SIE and November and December IWV and TT, over the period 1979 – 2016. We perform the analysis both in phase as well as with 1-month lag (IWV and TT leading the regional SIE index) to have a clear picture of the relationship between SIE and IWV and TT. We opted for November IO SIE and December RS SIE due to the fact that the highest SIE anomalies were recorded over these particular regions in 2016 (Figure S2 and Table 1).

The stability maps between November IO SIE and October/November IWV and TT are shown in Figures 5a-d, respectively. Based on the stable regions identified in Figures 5a-d we defined two indices: one for October IWV (IWV averaged over the yellow box in Figure 5a) and one for October TT (TT averaged over the yellow box in Figure 5c). For the in-phase stability maps (Figures 5b and 5d), the stable regions are very small and very regional and we did not considered them for further analysis. The correlation coefficient between November IO SIE and October IWV index is r = -0.62 (99% significance level), while the correlation coefficient between November IO SIE index and October TT index is r = -0.63 (99% significance level). In general, negative SIE anomalies over IO, in November, tend to occur in association with enhanced moisture and positive temperature anomalies over IO region in the previous month. In agreement with the findings in Section 3.3, year 2016 stands out as the most extreme one both in terms of SIE and moisture availability.

The stability maps between December WS SIE and November/December IWV and TT are shown in Figure 6a-d, respectively. In the case of December WS SIE, the stability maps show extended stable regions, having a dipole-like structure, both for November IWV and November TT. Positive SIE anomalies over WS, in December, are associated with negative IWV and TT anomalies over the WS region and positive IWV and TT anomalies over RS, in the previous November. Based on the stability maps in Figure 6a-d, we have defined five indices (yellow and green boxes in Figure 6a, 6c and 6d). As in the case of November IO, the stable regions are more extended for 1-month lag analysis. The correlation coefficient between December WS SIE and November IWV1 index is r = -0.68 (99% significance level) and the correlation between December WS SIE index and November TT1 index is r= -0.60 (99% significance level). The correlation coefficient between December WS SIE and November IWV2 (TT2) index is r = 0.34 (0.45), while the correlation coefficient between December WS SIE and December TT index is r = -0.35. Negative SIE anomalies, over WS in December, are occurring in association with enhanced moisture and positive temperature anomalies over the Weddell Sea and reduced moisture and negative temperature anomalies over RS, in the pervious month.

The significant lagged relationship between the regional SIE and previous month IWV and TT can be used as a potential predictive information for the development of the upcoming SIE over particular regions. The same analysis can be performed for other regions or at pan-Antarctic level and by including other climate/oceanic variables. Since the focus of our paper was to see the influence of the moisture and temperature on the development of the Antarctic sea ice extreme event in the austral spring of 2016, here we focused just on IWV and TT.

Earth Syst. Dynam. Discuss., https://doi.org/10.5194/esd-2017-114
Manuscript under review for journal Earth Syst. Dynam.
Discussion started: 18 December 2017

3.5 Daily evolution of the integrated water vapor transport in 2016

Based on the rank maps shown in Figure 3, we have defined there indices over the regions which rank as the wettest on record in October and November (black squares in Figure 3e and 3f). These indices have been computed by employing the daily integrated water vapor transport over the months of October and November from 1979 until 2016. The three region are define over ABS (Figure 7a), IO (Figure 7c), and WS (Figure 7e). Over ABS, the highest values of IWV, over the entire analyzed period, were recorded on 18th and 19th of October (Figure 7a). The vertically integrated total moisture transport shows a band of enhanced moisture stretching from the subtropical latitudes up to ABS (Figure 7b). Over the same period, there are two additional bands of enhanced moisture, with tropical origins, penetrating until IO and WPO. Over IO, the highest values of IWV in 2016 were recorded on 26th and 27th of October (Figure 7c). The vertically integrated total moisture transport shows a band of enhanced moisture stretching from the IO towards the coastal eastern part of Antarctica. One of the most intense events, in terms of IWV, took place on the 28th and 29th November 2016 (Figure 7e). Although the IWT index is defined over a restricted area in the RS, when looking at the vertically integrated total moisture transport, a very particular picture emerges. During this particular event, the RS and BAS were under the influence of the advection of moist and warm air from the tropical Pacific Ocean, IO received a band of enhanced moisture both from the Tropical South Atlantic Ocean as well as from the IO, and WPO received a lot of moisture from the IO. The combined effect of this enhanced moisture advection from the tropics, which happened simultaneously in ABS, RS, IO and WPO could, at least partly, explain the abrupt drop in the SIE in the first two weeks of December 2016. Looking at the daily vertically integrated total moisture transport, we can observe that moisture sources are coming from the tropical parts of the Pacific Ocean (for ABS and RS), Atlantic Ocean (for WS and IO), and Indian Ocean (for IO and WPO). This is in agreement with a recent study of Drumond et al. (2016), who show that the most important moisture sources for the Antarctic ice cores are: the subtropical South Atlantic Ocean, Indian Ocean, and South Pacific Ocean, depending on the location of the ice cores.

3.6 Southern Annular Mode and regional Antarctic sea ice

Given that the SAM has been associated with the trimming of the annual sea ice advance and retreat (Stammerjohn et al., 2008; Lefebre et al., 2004; Holland et al., 2017), in this sub-section we examine the regional response of the Antarctic sea ice, at monthly time scales, in relationship with SAM variability. Previous studies have shown that there is a regional response of the Antarctic sea ice to SAM-related forcings (Liu et al., 2004; Simpkins et al., 2012). Stammerjohn et al. (2008) have shown that changes in the western Antarctic Peninsula/southern Bellingshausen Sea and the western part of Ross Sea tend to occur with decadal changes in the mean state of SAM. Overall, the relationship between SAM and SIE is rather complicated (Marshall, 2003; Turner et al., 2013).

The focus of our analysis is on the months of September to December. For this, we have computed the correlation coefficients between the monthly regional SIE indices (ABS, IO, RS, WPO, and WS) and the monthly SAM index (Table 2). In September, significant correlations between SAM and regional SIE are found just for WS (r = -0.37, 95% significance level), while for the other regions, the correlations are not significant. Throughout the month of October, no significant

correlations are found between monthly SAM index and the regional Antarctic SIE, while for November significant correlations are found just between the SAM index and IO (r = 0.43, 99% significance level). In December, significant correlations are found between the SAM index and RS (r= 0.46, 99% significance level). As it can be inferred from Table 2, the relationship between SAM and the regional Antarctic SIE is rather non-stationary and varies from one month to the other. The Southern Annular Mode shows no statistically significant correlation with the SIE over ABS and WPO throughout September to December and significant correlations with IO, RS, and WS SIE just over particular months. Overall, positive SAM in September occurs in association with negative SIE anomalies over WS, while in November positive SAM tend to be associated with positive SIE over IO. In December, a positive SAM index is associated with positive SIE over RS. Although SAM can partly explain parts of the Antarctic sea ice variability (Stammerjohn et al., 2008), its influence on the sea ice variability over the Antarctic regions strongly depends on the considered month/season.

4 Discussion and conclusions

An initial attribution of the Antarctic conditions throughout the 2016 austral spring indicates that the atmospheric circulation in the Southern Hemisphere was very anomalous. The Southern Annular Mode was negative from October 2016 until December 2016, with top negative value of -3.12 in November 2016 (the fifth lowest SAM since 1958). The persistence of the negative phase of SAM throughout these three months led to a weakening of the circumpolar westerlies and an overall surface warming of the coastal parts of the Antarctic continent, as well as large parts inside the continent. The overall warming corroborated with enhanced poleward advection of warm and moist air led to strong sea ice melting, especially in October and November. Tietäväinen and Vihma (2008) have shown that northward water vapour transport, especially over the RS, WS, and IO, is usually associated with the SAM wave number three. This is in agreement with our findings, especially for the months of October and November 2016. As such, the exceptional water vapour transport in these two months could have been the result of extremely negative values of SAM, especially in November 2016.

Our study can be regarded as an additional piece on the puzzle regarding the drivers of the 2016 extremely low sea ice event over the Antarctic region. Turner et al. (2017) considered the spatial differences of the SIE anomalies and their temporal change at regional level and they related the low SIE over the Antarctic region to the warm air advection and the strong negative values of SAM in November and December. Schlosser et al. (2017) have shown that the rapid decrease in the sea ice area and extent were associated with atmospheric flow patterns reminiscent to a positive zonal wave number 3 (ZW3) index. The strong meridional flow associated with a positive ZW3 index triggered accelerated sea ice decline, especially at the beginning of November. From a pre-conditioning point of view, Stuecker et al. (2017) showed that the extreme low SIE in November-December 2016 was partially driven by the 2015/16 El-Niño event and the negative phase of SAM. In our study, we show that enhanced moisture and positive temperature anomalies over different parts of the Antarctic region (e.g. IO, WS, RS) could have also lead to the extremely low SIE recorded throughout the austral spring 2016. In October and November 2016, when the lowest daily SIC anomalies were observed, repeated episodes of poleward advection of warm and

moist air took place, with the most intense episode occurring at the end of November 2016. Moreover, October 2016 ranks as the wettest and warmest October over the last 39 years, over large areas in the IO, ABS and RS (Figure 3e and 3f), while November ranks as the wettest and warmest November over extended parts over WS, WP and WS (Figure 3h and 3i). In this study, we have shown that negative SIE anomalies at regional level (e.g. IO and WS) are preceded by enhanced moisture and positive temperature anomalies over these regions, one month ahead. The lagged relationship between the regional SIE anomalies and previous month IWV and TT could be used to provide a potential predictive skill for the upcoming development of the regional sea ice extent anomalies.

Although at Antarctic level no significant trends in the meridional moisture fluxes over the period 1979-2010 have been observed (Tsukernik et al., 2013), the austral spring 2016 stands out as very extreme in this respect, with 2016 ranking as the wettest (Figure S4a) and warmest austral spring on record (Figure S4b), over large areas covering Antarctica and the surrounding seas. The same holds for the Arctic region, boreal autumn 2016 ranking as the wettest and warmest autumn on record over almost the whole Arctic basin (Figure S4c and Figure S4d). Generally speaking, both austral spring and northern autumn 2016 have been characterized by enhanced poleward advection of moist and warm air. This exceptional event, occurring simultaneously in both polar regions, might be a direct or indirect consequence of the combined effect of 2015/16 El Niño event (Stuecker et al., 2017) and the fact that 2016, as a whole, was the warmest year on record (NOAA, 2017). Together, this two exceptional events could have triggered the release of large amounts of moist in the atmosphere and via particular large-scale atmospheric circulation patterns (e.g. Rossby waves, weaker jet stream), parts of this moisture have been carried out towards the poles.

From the perspective of future climate projection, these results imply that a realistic simulation of the Antarctic SIE trend requires also a proper simulation of both climate modes of variability (e.g. SAM) as well as extreme events (e.g. moisture intrusions, Rossby waves, atmospheric blocking). In recent study, Woods at al. (2017) have shown that the CMIP5 models agree reasonably well with the reanalysis in simulating the zonally integrated northward moisture flux, but have issues in properly simulating extreme southward moisture fluxes events.

Concluding, the 2016 austral spring event demonstrates that the present-day climate of the Antarctic continent and the surrounding areas allow for extensive sea ice reduction to occur. If such events are going to occur more frequently in the future is uncertain, but it is essential to understand and highlight the mechanisms responsible for triggering such events.

Acknowledgements. This study is promoted by Helmholtz funding through the Polar Regions and Coasts in the Changing Earth System (PACES) program of the AWI. Funding by the Helmholtz Climate Initiative REKLIM is gratefully acknowledged.

References

Bracegirdle, T. J., and G. J. Marshall (2012), The reliability of Antarctic tropospheric pressure and temperature in the latest global reanalyses, J. Clim., (25), 7138–7146.

Collins, M., and Coauthors (2014), Long-term climate change: Projections, commitments and irreversibility. Climate Change 2013: The Physical Science Basis, T. F. Stoker et al., Eds., Cambridge University Press, 1029-1136.

Comiso, J. C., *and* F. Nishio *(*2008). Trends in the sea ice cover using enhanced and compatible AMSR-E, SSM/I, and SMMR data, J. Geophys. Res., 113, *C02S07*, *doi:*10.1029/2007JC004257

Dee, D.P., et al. (2011), The ERA-interim reanalysis: Configuration and performance of the data assimilation system, Q. J. R. Meteorol. Soc., 137, 553–597.

Drumond, A., E. Taboada, R. Nieto, L. Gimeno, S.M. Vicente-Serrano, and J.I. López-Moreno (2016), A Lagrangian analysis of the present-day sources of moisture for major ice-core sites, Earth Syst. Dynam., 7, 549-558, https://doi.org/10.5194/esd-7-549-2016.

Fetterer, F., K. Knowles, W. Meier, and M. Savoie, (2016), *Sea Ice Index, Version 2*. Boulder, Colorado USA. NSIDC: National Snow and Ice Data Center. doi: http://dx.doi.org/10.7265/N5736NV7.

Grosfeld, K. et al. (2016), Online sea-ice knowledge and data platform <www.meereisportal.de> , Polarforschung, Bremerhaven, Alfred Wegener Institute for Polar and Marine Research & German Society of Polar Research, 85 (2), pp. 143-155 . doi: 10.2312/polfor.2016.011.

Holland, M.M., Landrum, L., Kostov, Y. et al. Clim Dyn (2017) 49: 1813. https://doi.org/10.1007/s00382-016-3424-9

Ionita, M., L.M. Tallaksen, D.G. Kingston, J.H. Stagge, G. Laaha, H.A.J. Van Lanen, P. Scholz, S. Chelcea, and K. Haslinger (2017), The European 2015 drought from a climatological perspective, Hydrol. Earth Syst. Sci., 21, 1397-1419, https://doi.org/10.5194/hess-21-1397-2017.

Ionita, M., M. Dima, G. Lohmann, P. Scholz and N. Rimbu (2014), Predicting the June 2013 European Flooding based on Precipitation, Soil Moisture and Sea Level Pressure. *J. Hydrometeorology*, 16, 598–614., doi: http://dx.doi.org/10.1175/JHM-D-14-0156.1

Ionita, M., G. Lohmann and N. Rimbu (2008), Prediction of Elbe discharge based on stable teleconnections with winter global temperature and precipitation, *Journal of Climate*, **21**, 6215–6226, doi:10.1175/2008JCLI2248.1

Ionita, M., 2017: Mid range forecasting of the German Waterways streamflow based on hydrologic, atmospheric and oceanic data, Reports on polar and marine research, Bremerhaven, Alfred Wegener Institute for Polar and Marine Research, 711 , 81 pp.

Jacobs, S.S., and J.C. Comiso (1997), Climate variability in the Amundsen and Belingshausen Seas, J. Clim., 10, 697-709.

Keller, L.M., S. Colwell, M.A. Lazzara, and R.L. Fogt, Eds., 2017: Antarctica – Surface Obervations (in "State of the Climate in 2016"). *Bull. Amer. Meteor. Soc.*, 98 (8), S158–S160.

Lefebvre, W., H. Goosse, R. Timmermann, *and* T. Fichefet *(*2004*),* Influence of the Southern Annular Mode on the sea ice–ocean system, J. Geophys. Res., 109, *C09005, doi:*10.1029/2004JC002403.

Lefebvre, W., and H. Goosse, (2005), Influence of the Southern Annular Mode on the sea ice-ocean system; The role of the thermal and mechanical forcing. Ocean Sci., 1, 145-157.

Liu, J.P, and J.A Curry (2010), Accelerated warming of the Southern Ocean and its impacts on the hydrological cycle and sea ice. Proc. Natl. Acad. Sci. USA, 107, 14987-14992.

Liu, J.P., J.A. Curry, and D.G. Martinson (2004), Interpretation of recent Antarctic sea ice variability. Geophys. Res. Lett., 31, L02205.

Marshall, G. J. (2003), Trends in the Southern Annular Mode from observations and reanalyses, J. Clim., 16, 4134–4143.

Meehl G.A., J.M. Arblaster, C.M. Bitz, C.T.Y. Chung, and H. Teng (2016**),** Antarctic sea-ice expansion between 2000 and 2014 driven by tropical Pacific decadal climate variability. *Nature Geoscience*, DOI: 10.1038/NGEO2751

Meier, W., F. Fetterer, M. Savoie, S. Mallory, R. Duerr, *and* J. Stroeve *(*2013*)* NOAA/NSIDC Climate Data Record of Passive Microwave Sea Ice Concentration, Version 2, 1979-2011, *Natl. Snow and Ice Data Cent., Boulder, Colo., doi:10.7265/N55M63M1*.

Meißner, D., Klein, B., and Ionita, M. (2017) Development of a monthly to seasonal forecast framework tailored to inland waterway transport in Central Europe, *Hydrol. Earth Syst. Sci. Discuss*., 2017, 1-31, doi:10.5194/hess-2017-293.

National Research Council (2012), *Seasonal to Decadal Predictions of Arctic Sea Ice: Challenges and Strategies*. Washington, DC: The National Academies Press. https://doi.org/10.17226/13515.

NOAA, (2017), National Centers for Environmental information, Climate at a Glance: Global Time Series, published February 2017, retrieved on March 11, 2017 from http://www.ncdc.noaa.gov/cag/

Parkinson, C.L., and D.J. Cavalieri (2012), Antarctic sea ice variability and trends, 1979–2010. The Cryosphere 6(4):871-880, doi: 10.5194/tc-6-871-2012.

Rayner, N. A., D.E. Parker, E.B. Horton, C.K. Folland, L.V. Alexander, D.P. Rowell, E.C. Kent, and A. Kaplan (2003), Global analyses of sea surface temperature, sea ice, and night marine air temperature since the late nineteenth century J. Geophys. Res.Vol. 108, No. D14, 4407 10.1029/2002JD002670

Schlosser, E., Haumann, F. A., and Raphael, M. N. (2017), Atmospheric influences on the anomalous 2016 Antarctic sea ice decay, The Cryosphere Discuss., https://doi.org/10.5194/tc-2017-192, in review.

Serreze, M.C., M.M. Holland, and J. Stroeve (2007), Perspectives on the Arctic's shrinking sea-ice cover. Science 315(5818):1533–1536.

Serreze, M.C., and J. Stroeve (2015), Arctic sea ice trends, variability and implications for seasonal ice forecasting. Philos Trans A Math Phys Eng Sci. 2015 Jul 13; 373(2045): 2014015

Shu, Q., Z. Song, and F. Qiao (2015), Assessment of sea ice simulations in the CMIP5 models, The Cryosphere, 9, 399-409, https://doi.org/10.5194/tc-9-399-2015.

Simpkins, G.R., L.M. Ciasto, D.W. Thompson, and M.H. England (2012), Seasonal Relationships between Large-Scale Climate Variability and Antarctic Sea Ice Concentration. *J. Climate*, **25**, 5451–5469, https://doi.org/10.1175/JCLI-D-11-00367.1

Stammerjohn, S.E., D.G. Martinson, R.C. Smith, X. Yuan, and D. Rind (2008), Trends in Antarctic annual sea ice retreat and advance and their relation to El Niño-Southern Oscillation and Southern Annular Mode variability. *J. Geophys. Res.*, **108**, C03S90, doi:10.1029/2007JC004269.

Stammerjohn, S.E., R. Massom, D. Rind, and D.G. Martinson (2012), Regions of rapid sea ice change: An inter-hemispheric seasonal comparison, Geophys. Res. Lett., 39, L06501.

Stammerjohn, S.E., and T. Scambos, Eds., 2017: Antarctica (in "State of the Climate in 2016"). *Bull. Amer. Meteor. Soc.*, **98** (8), S155–S172.

Stroeve, J., V. Kattsov, A. Barrett, M. Serreze, T. Pavlova, M. Holland, and W. Meier (2012), Trends in Arctic sea ice extent from CMIP5, CMIP3 and observations, Geophys. Res. Lett., 39, L16502, doi:10.1029/2012GL052676.

Stroeve, J. et al.. (2015), Improving predictions of Arctic sea ice extent. *Eos*, *96*. doi:10.1029/2015EO031431.

Stuecker, M. F., C. M. Bitz, and K.C. Armour (2017), Conditions leading to the unprecedented low Antarctic sea ice extent during the 2016 austral spring season. Geophys. Res. Lett., 44, 9008–9019, *doi:*10.1002/2017GL074691.

Tietäväinen, H., and T. Vihma (2008), Atmospheric moisture budget over Antarctica and the Southern Ocean based on the ERA-40 reanalysis. Int. J. Climatol., 28: 1977–1995. doi:10.1002/joc.1684

Tsukernik, M., and A.H. Lynch (2013), Atmospheric Meridional Moisture Flux over the Southern Ocean: A Story of the Amundsen Sea. *J. Climate*, **26**, 8055–8064, https://doi.org/10.1175/JCLI-D-12-00381.1

Turner, J., T. Phillips, G.J. Marshall, J.S. Hosking, J.O. Pope, T.J. Bracegirdle, *and* P. Deb *(*2017*)*, Unprecedented springtime retreat of Antarctic sea ice in 2016, Geophys. Res. Lett., 44, 6868–6875, *doi:10.1002/2017GL073656.*

Turner, J. et al. 2009: Non-annular atmospheric circulation change induced by atmospheric ozone-depletion and its role in the recent increase of Antarctic sea ice extent. Geophys. Res. Lett., 36, L08502

Turner, T., J. Bracegirdle, T. Phillips, G.J. Marshalll, and J.S. Hoskins (2013), An initial assessment of Antarctic sea ice extent in the CMIP5 models. J. Climate, 26, 1473-1484, doi:10.1175/JCLI-D-12-00068.1.

Woods, C., R. Caballero, and G. Svensson (2017) Representation of Arctic Moist Intrusions in CMIP5 Models and Implications for Winter Climate Biases. *J. Climate*, **30**, 4083–4102, https://doi.org/10.1175/JCLI-D-16-0710.1

Yuan N., M. Ding, J. Ludescher, and A. Bunde (2017) Increase of the Antarctic Sea Ice Extent is highly significant only in the Ross Sea. Sci Rep 7:41096.

Zhang, J. L., (2007) Increasing Antarctic sea ice under warming atmospheric and oceanic conditions, J. Clim., 20, 2515-2529.

Zwally, H. J., J.C. Comiso, C.L. Parkinson, D.J. Cavalieri, and P. Gloersen (2002), Variability of Antarctic sea ice 1979–1998, J. Geophys. Res., 107(C5), 3041, doi:10.1029/2000JC000733

Earth Syst. Dynam. Discuss., https://doi.org/10.5194/esd-2017-114
Manuscript under review for journal Earth Syst. Dynam.
Discussion started: 18 December 2017

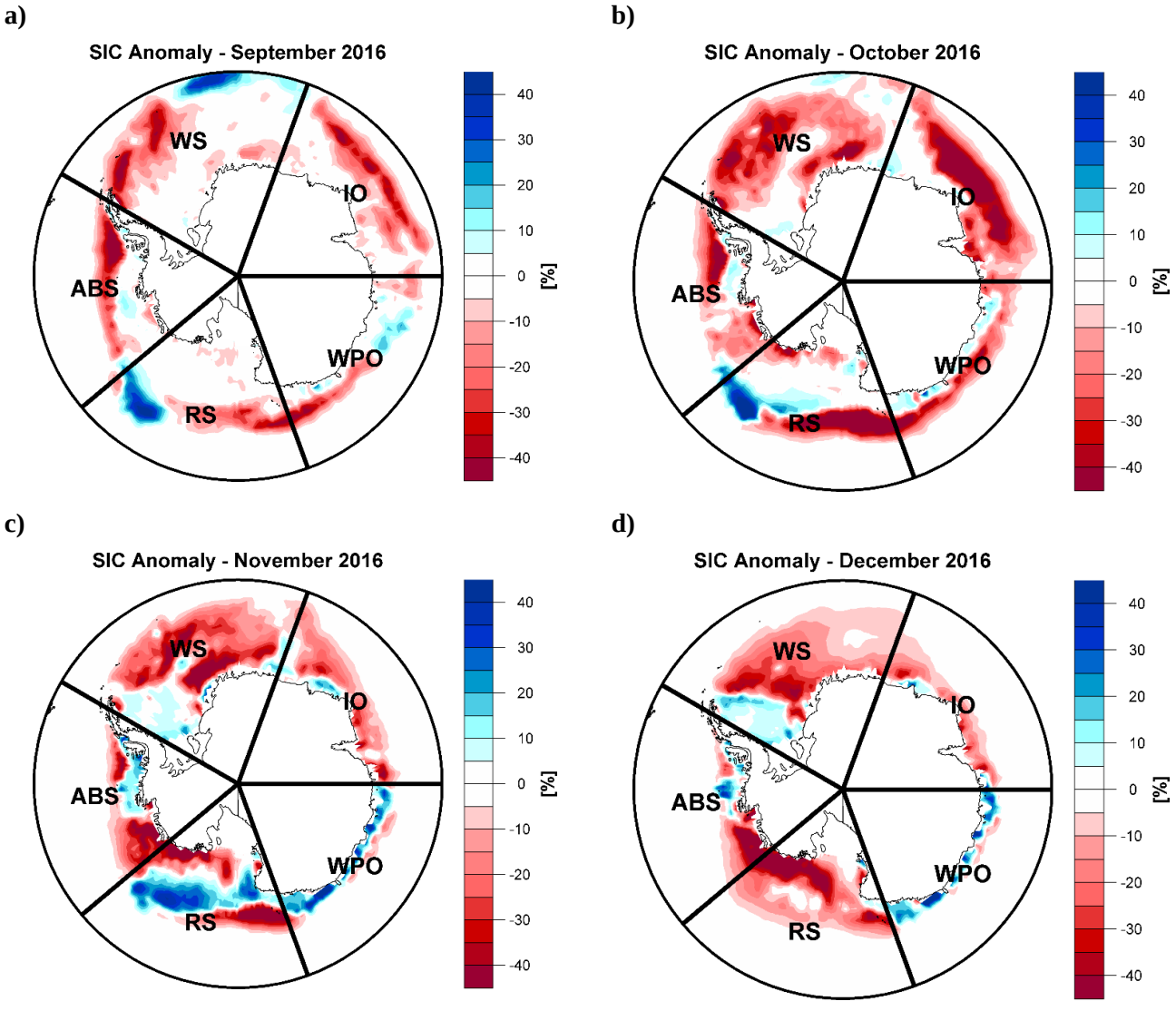

Figure 1. Sea Ice Concentration (SIC) anomalies for: a) September 2016; b) October 2016; c) November 2016 and d) December 2016. The anomalies are computed relative to the reference period 1979 – 2010. WS = Weddell Sea; IO = Indian Ocean; WPO = Western Pacific Ocean; RS = Ross Sea; ABS = Amundsen - Bellingshausen Sea.

Earth Syst. Dynam. Discuss., https://doi.org/10.5194/esd-2017-114
Manuscript under review for journal Earth Syst. Dynam.
Discussion started: 18 December 2017

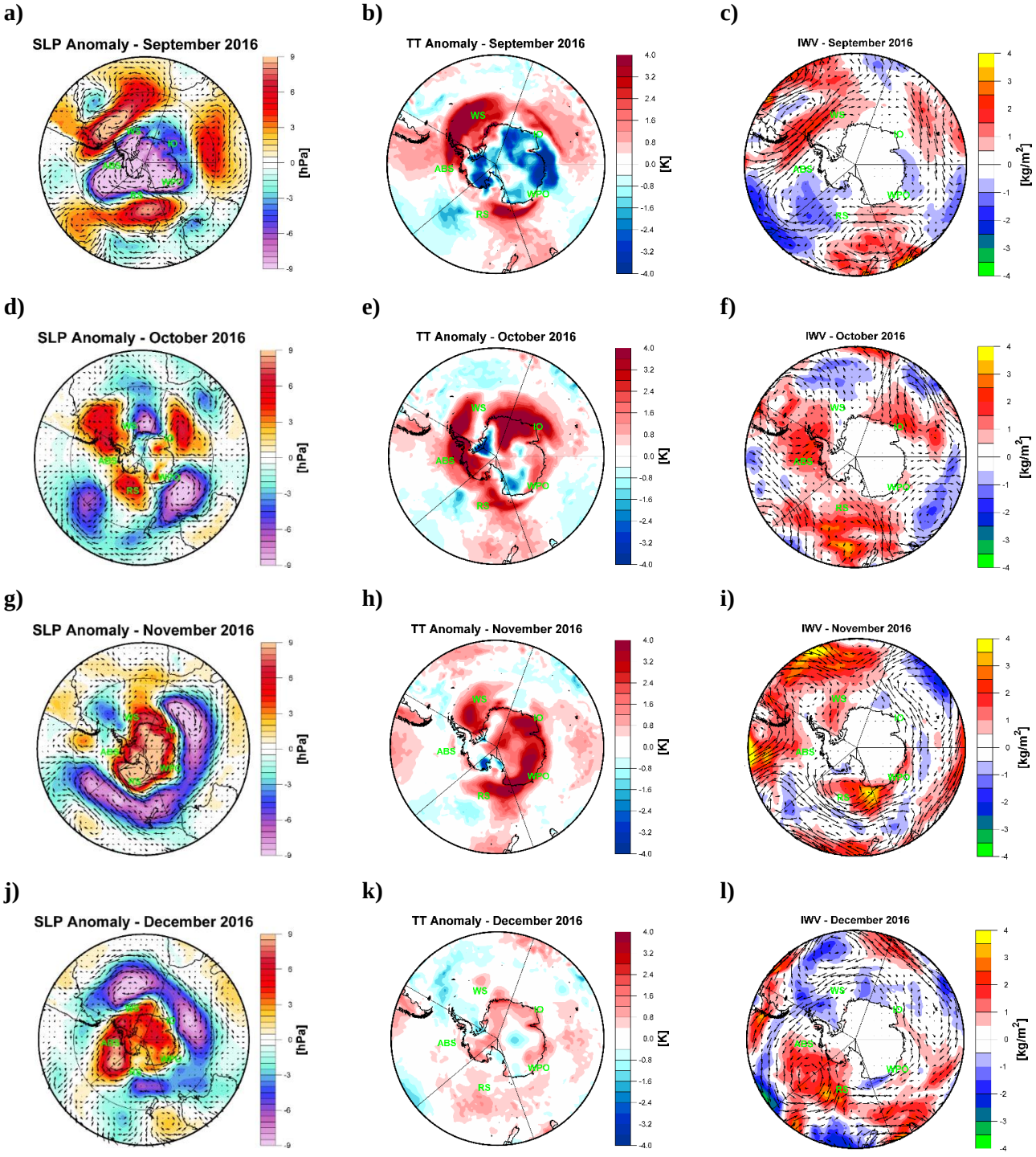

Figure 2. Sea level pressure (SLP) anomalies from September until December 2016 (first column), 2m air temperature (TT) anomalies from September until December 2016 (middle column) and water vapor transport (IWV) anomalies from September until December 2016 (last column). The anomalies are computed relative to the reference period 1979 – 2010.

Earth Syst. Dynam. Discuss., https://doi.org/10.5194/esd-2017-114
Manuscript under review for journal Earth Syst. Dynam.
Discussion started: 18 December 2017

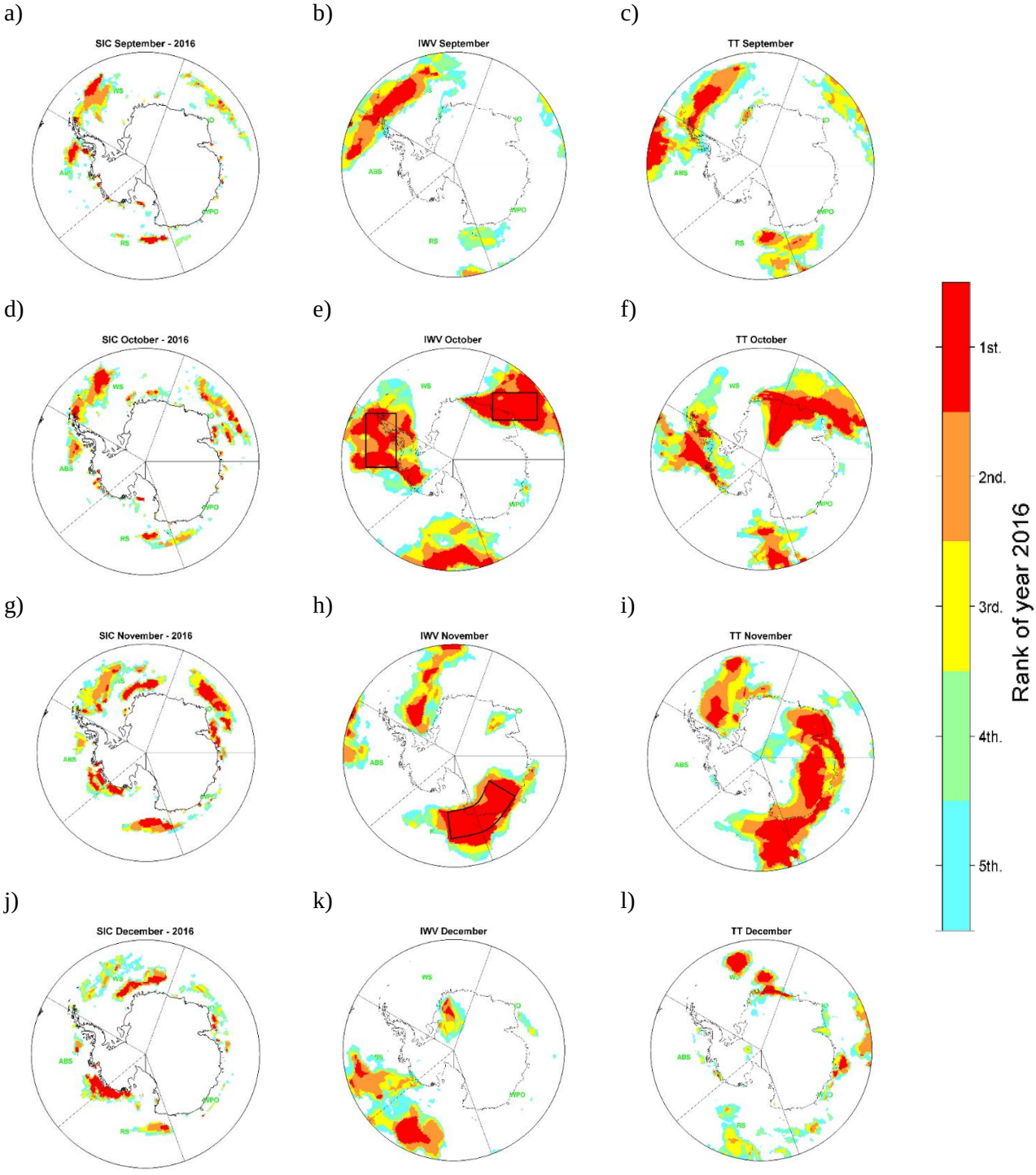

Figure 3. Top-five ranking of 2016 monthly lowest sea ice concentration (SIC) (first column), top-five ranking of 2016 wettest month (middle column) and), top-five ranking of 2016 warmest month (third column). 1 means the lowest SIC/wettest/warmest month since 1979, 2 signifies the second lowest SIC/wettest/warmest, etc. Analyzed period: 1979–2016.

Earth Syst. Dynam. Discuss., https://doi.org/10.5194/esd-2017-114
Manuscript under review for journal Earth Syst. Dynam.
Discussion started: 18 December 2017

Earth System Dynamics
Discussions
Open Access
EGU

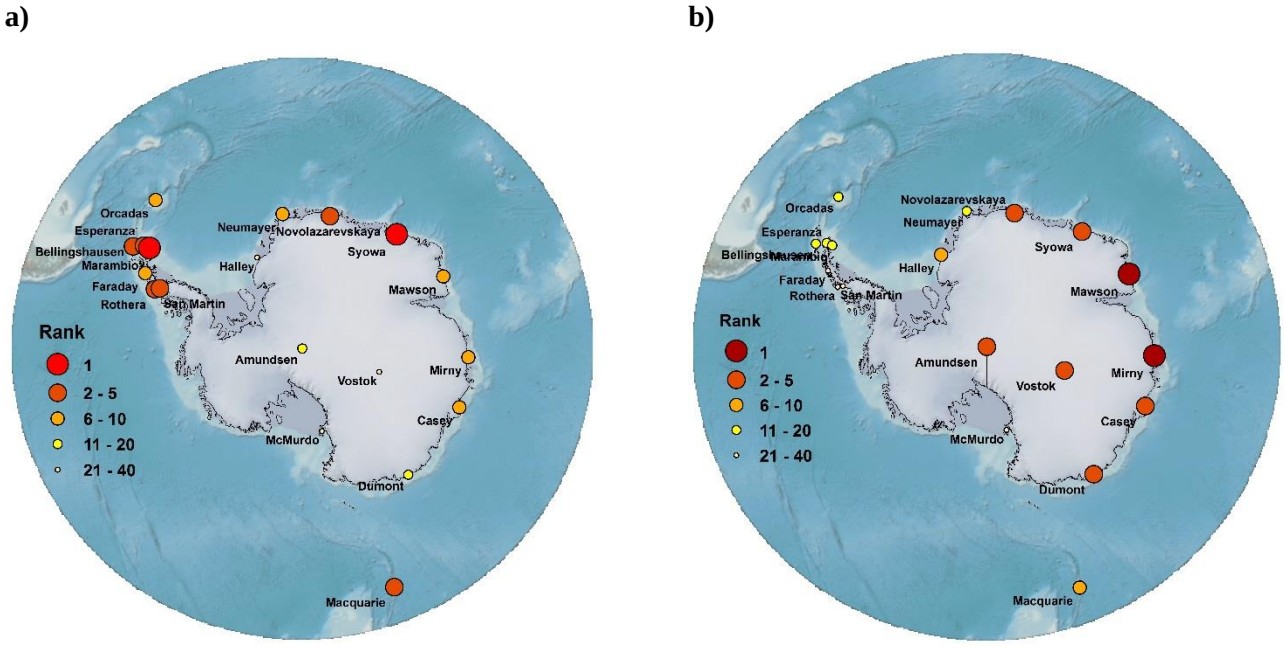

Figure 4. Ranking of the monthly mean temperature at observation stations: a) October 2016 and b) November 2016. 1 means the warmest month since 1981, 2 signifies the second warmest, etc. Analyzed period: 1981–2016.

Earth Syst. Dynam. Discuss., https://doi.org/10.5194/esd-2017-114
Manuscript under review for journal Earth Syst. Dynam.
Discussion started: 18 December 2017

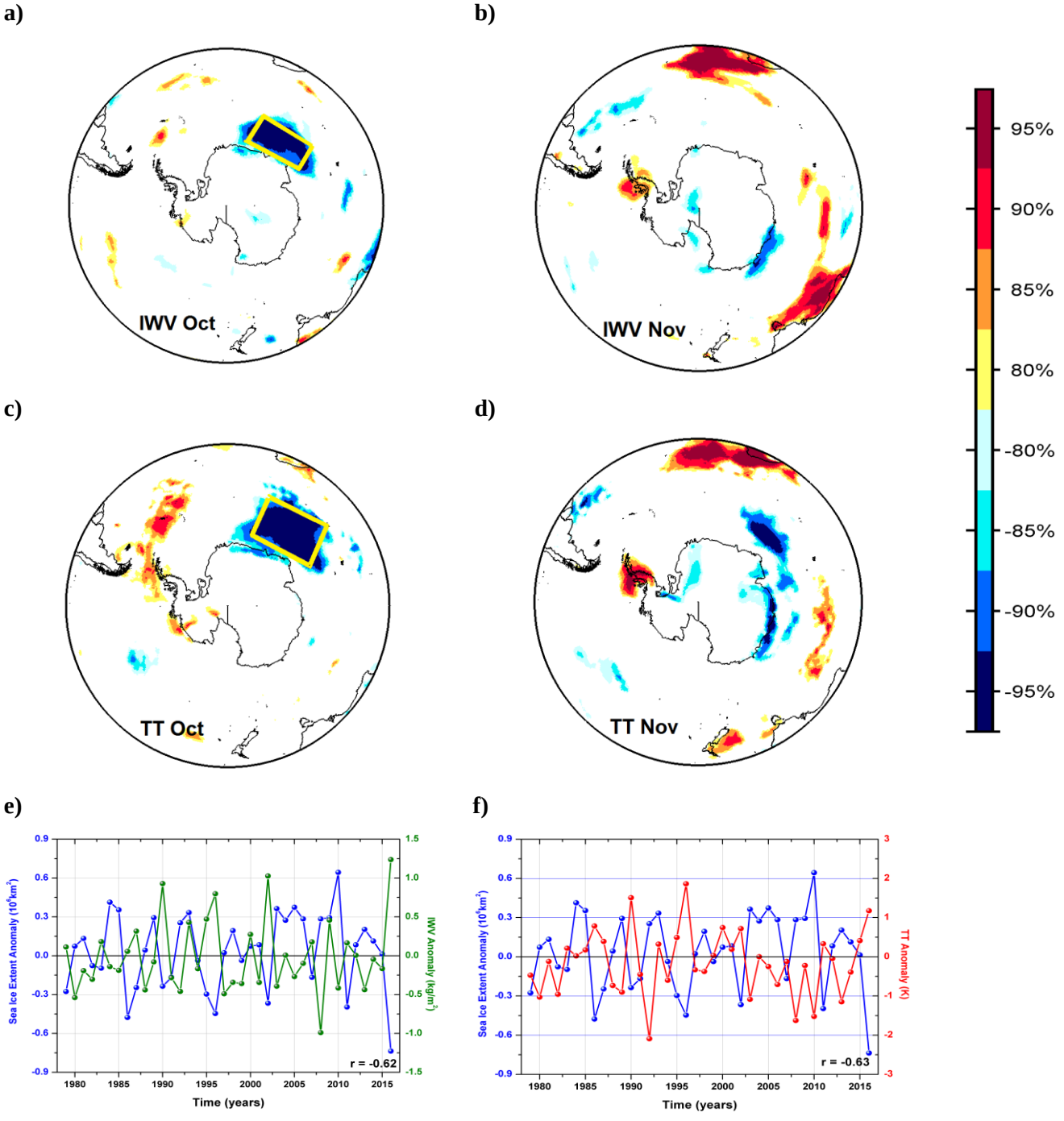

Figure 5. a) The stability map between November IO Sea Ice Extent and October IWV; b) The stability map between November IO Sea Ice Extent and November IWV; c) The stability map between November IO Sea Ice Extent and October TT; d) The stability map between November IO Sea Ice Extent and November TT; e) The time series of November IO Sea Ice Extent (blue line) and the time series of October IWV (green line) averaged over the yellow box in a); f) The time series of November IO Sea Ice Extent (blue line) and the time series of October TT (red line) averaged over the yellow box in c).

Earth Syst. Dynam. Discuss., https://doi.org/10.5194/esd-2017-114
Manuscript under review for journal Earth Syst. Dynam.
Discussion started: 18 December 2017

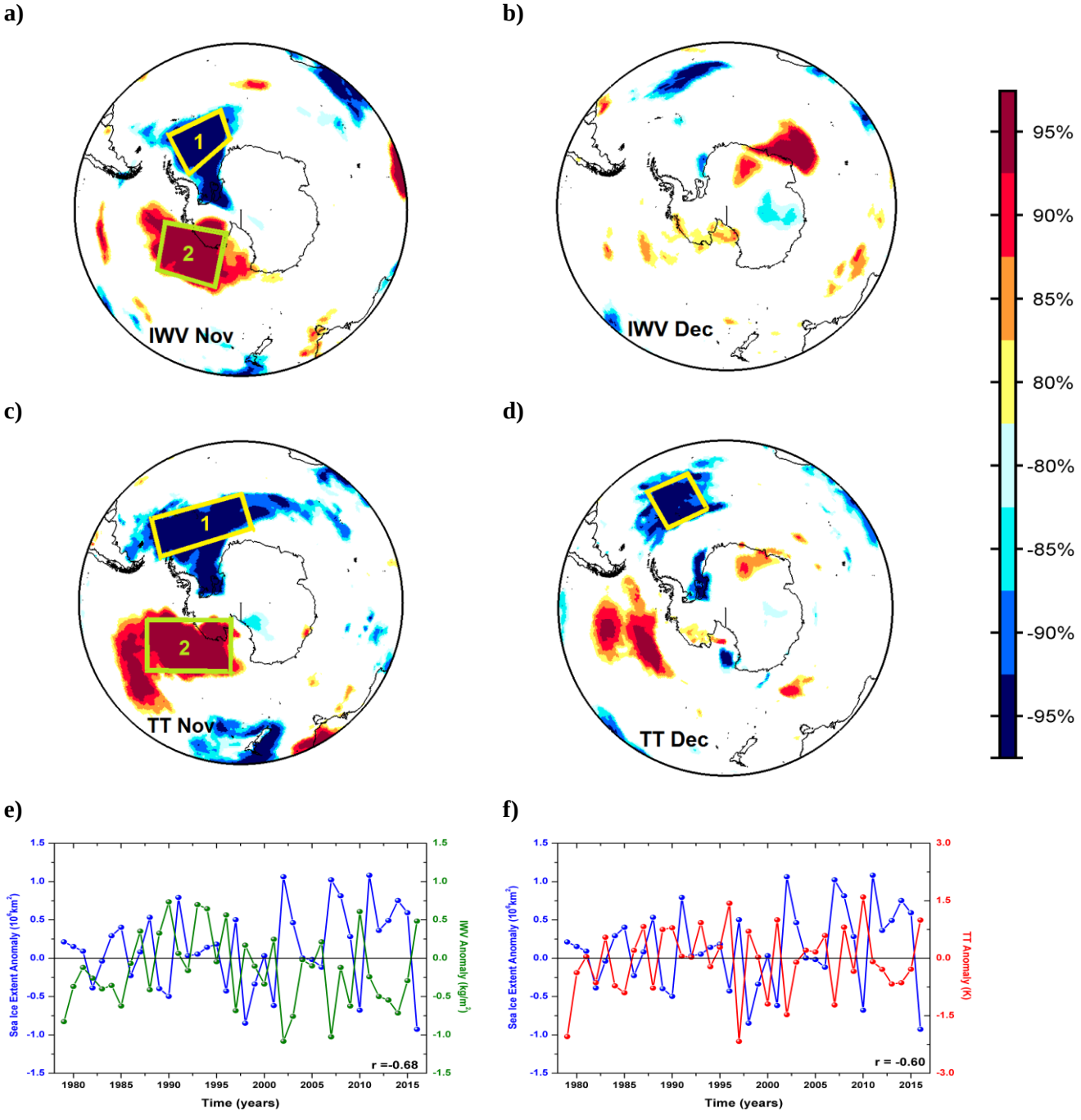

Figure 6. a) The stability map between December WS Sea Ice Extent and November IWV; b) The stability map between December WS Sea Ice Extent and December IWV; c) The stability map between December WS Sea Ice Extent and November TT; d) The stability map between December WS Sea Ice Extent and December TT; c) The time series of December WS Sea Ice Extent (blue line) and the time series of November IWV1 (green line) averaged over the yellow box in a); c) The time series of December WS Sea Ice Extent (blue line) and the time series of November TT1 (red line) averaged over the yellow box in b).

Earth Syst. Dynam. Discuss., https://doi.org/10.5194/esd-2017-114
Manuscript under review for journal Earth Syst. Dynam.
Discussion started: 18 December 2017

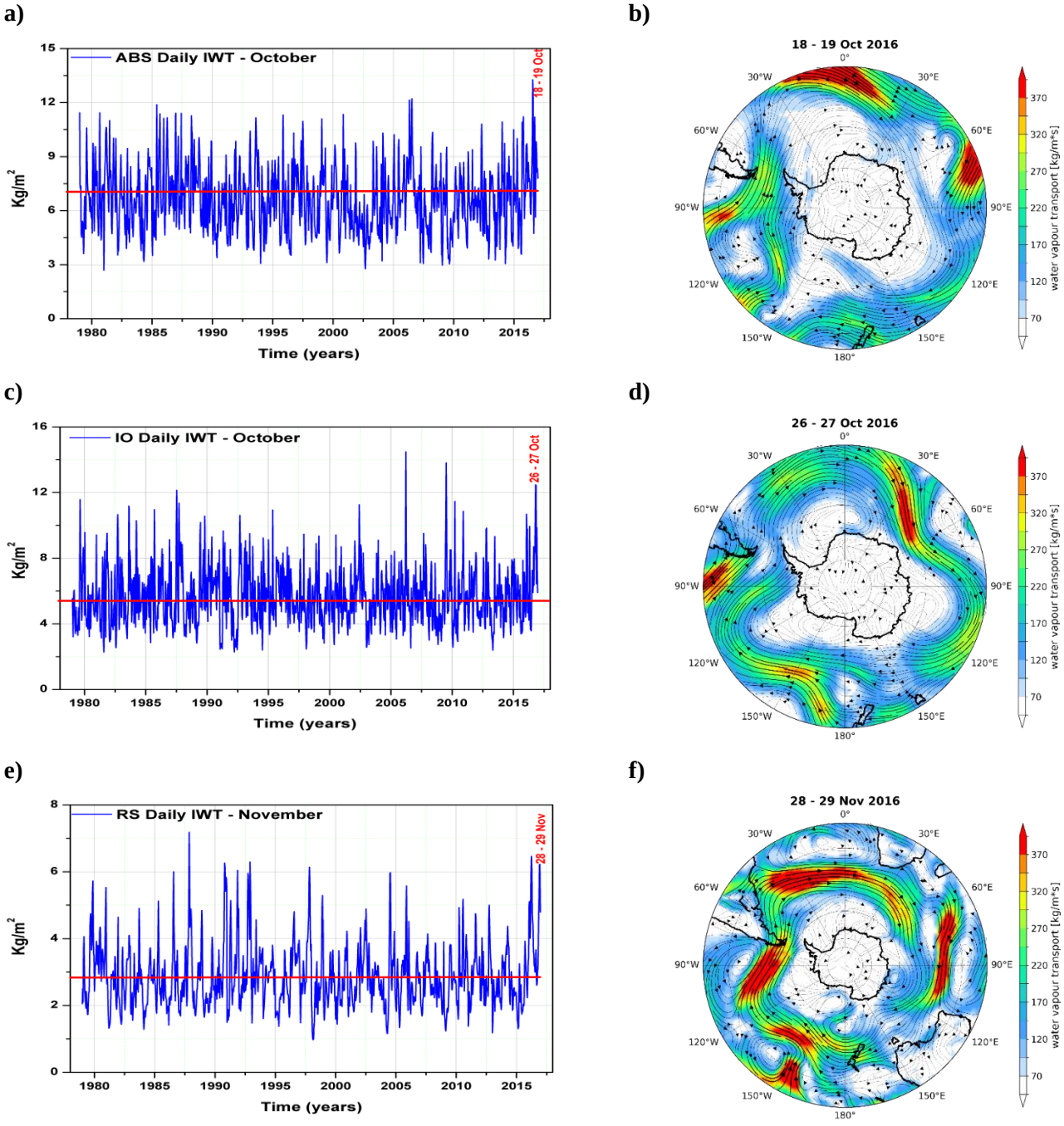

Figure 7. a) Daily IWT averaged over ABS (black square in Figure 3e) over the period 1979 – 2016; b) The vertically integrated total moisture transport on the 18-19th October 2016; c) Daily IWT averaged over IO (black square in Figure 3e) over the period 1979 – 2016; d) Vertically integrated total moisture transport on the 26-27th October 2016; e) Daily IWT averaged over RS (black square in Figure 3h) over the period 1979 – 2016 and f) Vertically integrated total moisture transport on the 28-29th November 2016.

Earth Syst. Dynam. Discuss., https://doi.org/10.5194/esd-2017-114
Manuscript under review for journal Earth Syst. Dynam.
Discussion started: 18 December 2017

Earth System Dynamics Discussions Open Access EGU

Table 1. Rank of regional Sea Ice Extent from September to December 2016.

	September	**October**	**November**	**December**
ABS	5	4	8	4
IO	2	2	**1**	2
RS	10	2	**1**	2
WP	15	11	**1**	22
WS	32	27	12	**1**
ANT	3	2	**1**	**1**

Earth Syst. Dynam. Discuss., https://doi.org/10.5194/esd-2017-114
Manuscript under review for journal Earth Syst. Dynam.
Discussion started: 18 December 2017

Earth System Dynamics Discussions Open Access EGU

Table 2. Correlation coefficients between regional sea ice extent and monthly Sothern Annular Mode

	September	**October**	**November**	**December**
ABS	0.21	0.23	0.09	0.10
IO	0.07	0.17	**0.43****	0.31
RS	-0.25	-0.03	0.05	**0.46****
WPO	0.04	0.07	0.05	0.16
WS	**-0.37***	-0.29	-0.13	0.20

* 95% significance level

** 99% significance level